ISTANBUL TECHNICAL UNIVERSITY ★ GRADUATE SCHOOL OF SCIENCE ENGINEERING AND TECHNOLOGY

DYNAMIC INVESTIGATION OF STICK-SLIP OSCILLATIONS ON A TRANSLATING FRICTION BAND

M.Sc. THESIS

Anıl ŞENGÜLER

Department of Mechanical Engineering

Automotive Engineering Program

NOVEMBER 2015

ISTANBUL TECHNICAL UNIVERSITY ★ GRADUATE SCHOOL OF SCIENCE ENGINEERING AND TECHNOLOGY

DYNAMIC INVESTIGATION OF STICK-SLIP OSCILLATIONS ON A TRANSLATING FRICTION BAND

M.Sc. THESIS

Anıl ŞENGÜLER
(503121703)

Department of Mechanical Engineering

Automotive Engineering Program

Thesis Advisor: Dr. Osman Taha ŞEN

NOVEMBER 2015

İSTANBUL TEKNİK ÜNİVERSİTESİ ★ FEN BİLİMLERİ ENSTİTÜSÜ

YAPIŞMA-KAYMA SALINIMLARININ SÜRTÜNME BANDI ÜZERİNDE DİNAMİK İNCELENMESİ

YÜKSEK LİSANS TEZİ

Anıl ŞENGÜLER
(503121703)

Makina Mühendisliği Anabilim Dalı

Otomotiv Mühendisliği Programı

Tez Danışmanı: Dr. Osman Taha ŞEN

KASIM 2015

Anıl ŞENGÜLER, a **M.Sc.** student of ITU **Graduate School of Science Engineering and Technology** student ID 503121703, successfully defended the **thesis** entitled "**DYNAMIC INVESTIGATION OF STICK SLIP OSCILLATIONS ON A TRANSLATING FRICTION BAND**", which he prepared after fulfilling the requirements specified in the associated legislations, before the jury whose signatures are below.

Thesis Advisor :	**Dr. Osman Taha ŞEN** Istanbul Technical University	....
Jury Members :	**Prof. Dr. Ahmet GÜNEY** Istanbul Technical University	....
	Doç. Dr. Tarkan SANDALCI Yıldız Technical University	....

Date of Submission : 27 November 2015
Date of Defense : 25 December 2015

To my spouse and family,

FOREWORD

The main goal of this project is the observation of the groan initiation, which is a brake noise problem that occurs in mid-range frequencies. After completing literature research and building mathematical model, I was ready for building experimental set-up to investigate the stick-slip vibrations in brake system. I would like to thank Dr. Osman Taha Şen for his help and encouragement and mechanical engineering department and automotive division, OTAM for providing us the opportunity to make this research happen. I also would like to acknowledge ITU Scientific Research Program (Project no:38466) for funding this research project.

November 2015

Anıl ŞENGÜLER
Chassis Development Engineer

TABLE OF CONTENTS

Page

ABBREVIATIONS

App : Appendix
CoG : Center of Gravity
Fig : Figure

-

LIST OF TABLES

Page

LIST OF FIGURES

Page

DYNAMIC ANALYSIS OF STICK-SLIP OSCILLATIONS ON A TRANSLATING FRICTION BAND

SUMMARY

Brake noise and vibration, which is caused by the friction on the system, has been a problem since the creation of the brake system. Even though these problems do not influence human life directly, many researches are made to obtain more quiet and balanced systems. However, it has not been found a concrete solution yet because of the complex dynamical characteristics of brake systems.

The main goal of this thesis is to investigate the groan problem. Vehicle brake groan is a mid-frequency, friction-induced forced vibration problem. Brake groan problem occurs at very low speeds of brake systems, and undesired vibrations emerge at mid-frequency band such as 100-500 Hz. This project includes formulation, design, examination and evaluation to simulate brake groan problem. The major source mechanism to this problem is known as stick-slip vibrations that are led by several nonlinear effects, and the nonlinear characteristics of friction coefficient are believed to be the major source.

The literature review is made after thesis subject is specified. The various several articles are observed to obtain a better understanding on groan problem. After literature review, two following approaches are used in this project.

Firstly, a two degree of freedom nonlinear model is built according to the mathematical model. Since the governing equations is in the form of nonlinear equations, a single degree of freedom linear model of translating friction element is generated. The solutions for 6 cases which is specified in time domain will be obtained with generated numerical solution codes with the help of MATLAB software.

Secondly, experimental setup, which has components such as friction material, friction band, compressors, pneumatic cylinders etc., is designed with the help of CATIA software. This friction element, which is designed, includes two frictional guides and an actuator to simulate dynamic interactions between the brake pad and the calipers. After design stage, experimental process is completed. The measurement is done with the linear accelerometers which is replaced on the different sides on friction element. The data is collected, converted to digital inputs and transferred to the computer. The results are copied from Brüel&Kjaer software program to Excel. Then, the graphs in time domain are drawn with the help of MATLAB according to these results.

Finally, experimental and mathematical data are compared and discussed. The differences and similarities are tried to specifiy in conclusion section. The results are discussed and evaluated whether the predictions of both mathematical models correlate well or not.

KAYMA-YAPIŞMA SALINIMLARININ SÜRTÜNME BANDI ÜZERİNDE DİNAMİK İNCELENMESİ

ÖZET

Günümüz dünyasında, otomobil, otobüs ve kamyon vb. kara araçları, yüzeyler arasındaki sürtünmeden yararlanıp; sahip olduğu kinetik enerjiyi ısı enerjisine çevirerek frenleme yapmaktadır. Fren sistemlerindeki sürtünmeden kaynaklanan fren titreşim ve gürültü problemleri, bu sistemlerin icadından beri problem teşkil etmektedir. Bu durum insan hayatını doğrudan etkilemese bile, daha sessiz ve dengeli sistemler elde etme isteğinden ötürü, bu konuyla ilgili pek çok araştırma yapılmıştır. Fren sistemlerinin komplike dinamik karakteristiklerinden dolayı henüz ortaya kesin bir çözüm konulamamıştır.

Bu projenin asıl amacı, groan problemini incelemektir. Fren groan problemi, frenleme esnasında araç yavaşça durdurulduğunda veya kalkış esnasında araç yavaşça hareket ettirildiğinde meydana gelir. Fren sistemlerindeki titreşimler, yüksek, orta ve düşük frekanslı titreşimler olarak gruplandırılmaktadır. Fren groan problemi, orta frekanslı titreşim kaynaklı bir gürültü problemidir. Fren groan problemi, düşük hızlarda meydana gelir, 100-500 Hz. lik orta frekans aralığında rahatsız edici bir gürültü şeklinde ortaya çıkar. Bu proje matematik model formülasyonu, deney sistemi dizaynı, fren groan probleminin gözlemlenmesini ve değerlendirilmesini içermektedir. Bu problemin ana kaynağı olarak, çeşitli lineer olmayan etkilerden oluşan yapışma-kayma salınımları ve sürtünme katsayısının lineer olmayan karakteristiği düşünülmektedir. Tezin konusu olarak da groan problemine sebebiyet veren yapışma-kayma salınımlarının incelenmesi seçilmiştir.

Tezin konusu saptandıktan sonra, groan problemini anlamak, problemin detaylarına hakim olmak maksadıyla literatür araştırmasına geçilmiştir. Farklı konu başlıklı makaleler problem daha iyi anlayabilmek için irdelenmiştir. Literatür araştırması, tez için gerekli olan matematik modelin kurulmasına olanak sağlamıştır. Literatür araştırmasından sonra, bu projede aşağıda bahsedilen deneysel ve matematiksel yaklaşımlar kullanılmıştır. Matematik modelden yola çıkılarak, numerik çözümler ile deney tertibatı oluşturulmuştur. Matematik modelde farklı iki tip kaliper modeli bulunmaktadır. Bunlardan bir tanesi sürtünme bağlantısının trailing ucunda olduğu itmeli tip kaliperdir. Diğeri ise sürtünme bağlantısının leading ucunda olduğu çekmeli tip kaliperdir. Her iki yaklaşım da, itmeli ve çekmeli tip diye adlandırılan farklı iki tip kaliperin, iki farklı uç noktalarına ve merkezlerine normal yükler uygulanarak ve bunun sonucunda elde edilen verilerin incelenmesini içermektedir

İlk olarak, matematik modele göre iki serbestlik dereceli lineer olmayan model kurulmuştur. Bu sistemde, dönme ve öteleme olmak üzere toplamda iki adet serbestlik derecesi mevcuttur. Elde edilen denklemler sistemin doğası gereği lineer olmadıkları için, sürtünme elemanının bir serbestlik dereceli modeli oluşturulmuştur. 6 farklı kıstas için numerik kodlar yazılmıştır. Bu kıstaslar, sırasıyla, itmeli kaliperde normal yükün merkezde, leading ucunda, trailing ucundan normal kuvvetlerin

etkidiği ve diğer tip kaliper olan çekmeli kaliperde normal yükün merkezde, trailing ve leading ucunda olduğu durumlardır. Nümerik kodlar üç farklı durum göz önünde bulundurularak oluşturulmuştur. Bunlardan bir tanesi, pad yani balata hızının, band hızına yani disk hızına eşit olduğu durumdur. İkinci durum, padin banttan daha hızlı olduğu durumdur. Son durum ise, padin banttan yavaş olduğu durumdur. MATLAB üzerinden bulunan sonuçlar grafiklere zaman tanım kümesinde dökülmüştür. Bu grafikler 6 farklı kıstasa göre sırasıyla yer değiştirme-zaman, hız-zaman, açısal yer değiştirme-zaman ve açısal hız-zaman grafikleridir. Bu grafiklerin içerisindeki tepe noktaları arasındaki farktan yararlanılarak, her iki kaliper tipi için 6 farklı durumu anlatan değerler tablo halinde bölüm sonunda özetlenmiştir.

İkinci olarak, sürtünme materyali, sürtünme bandı, kompresör ve pnömatik silindirlerden oluşan deney düzeneği CATIA yardımıyla dizayn edilmiştir. Sürtünme materyali, fren balatasını temsil etmektedir. Sürtünme malzemesi, eski bir araçtan alınmıştır. Sürtünme bandı ise fren diskini temsil etmektedir. Sürtünme bandı, alüminyum sac malzemeden işlenerek elde edilmiştir. Pnömatik silindirlerden bir tanesi, sürtünme bandına hareket vermek için düşünülmüştür. Diğer pnömatik silindir ise, normal yükün istenilen farklı noktalara etki etmesini sağlamak için seçilmiştir. Bu pnömatik silindir sayesinde etki alanı değiştirilerek istenilen 6 farklı kıstas sağlanmaktadır. Kısacası, dizayn edilen sürtünme elemanı, fren balatası ve kaliperi arasındaki etkileşimleri simule etmek için, iki pivot nokta ve aktüatörden oluşmaktadır. Deney tertibatı, hem itmeli hem de çekmeli kalipere adapte olacak şekilde düşünülmüştür.

Dizayn aşamasından sonra deney işlemine geçilmiştir. Deney tertibatı hava sistemi, elektriksel sistem ve mekanik sistem olmak üzere üç ana kategoriden oluşmaktadır. Hava sistemi, hava hortumları, pnömatik silindirler, t bağlantılar, iğne valfleri, bağlantı elemanları, manometreler ve açma kapama vanalarından oluşmaktadır. Elektrik sistem için ise güç besleme ünitesi ve veri toplama sistemleri gerekmektedir. Mekanik sistem ise sürtünme malzemesi, sürtünme bandı, L braketler, montajlı braketler, cıvatalar, somunlar, destekleme plakası ve teflon plakadan oluşmaktadır. Deney esnasında pnömatik silindir yardımıyla sürtünme materyalinin sürtünme bandı üzerinde kayması sağlanmaktadır.

Sürtünme elemanının farklı bölgelerine konulan lineer ivme ölçerler sayesinde ölçümler yapılmıştır. İvme ölçerlerden bir tanesi diskin x yönündeki ivmesini ölçmek maksadıyla sürtünme bandı üzerine konulmuştur. Diğer bir ivme ölçer ise balatanın x yönündeki ivmesini ölçmek için sürtünme malzemesi üzerine yerleştirilmiştir. Diğer ivme ölçerler y eksenindeki ivmelenmeyi görmek için sürtünme materyali üzerine yerleştirilmiştir. Bu ivme ölçerler sırasıyla trailing ve leading uçlarındaki y ekseni yönündeki değerleri elde etmek amaçlıdır. İvme ölçerler yüksek hassaslıktaki kablolarla veri toplama sistemine bağlıdır. Sistemde hareketin başlamasıyla birlikte verileri aktarma kabiliyetine sahiptir. Başlangıçta pnömatik silindirlere ait vanalar kapalıdır. Bu nedenle sistem içerisine hava girişi yoktur. Kompresörden yaklaşık 6 bar civarında bir hava girişi olmaktadır. Pnömatik silindirin vanası kullanılarak basınç değeri 5 bar olarak ayarlanır. İvme ölçerler çok hassas olduklarından sistem dışında meydana gelen en ufak bir titreşimden etkilenmektedirler. BU nedenle pnömatik sistemin basıncını ayarlamak, stabil sistem yaratmak, sürtünme bandının hareketini yavaş şekilde sağlamak için çok önemlidir. Pnömatik silindirden 0,6-0,7 bar arasında hava geldiğinde sürtünme bandı hareket etmeye başlamaktadır. Bir anda ani yüklenmeden ötürü sinyal, sistemin olması gerektiği gibi hareket edememesinden kaynaklanır. Bu sebepten, sistemi lineer, yavaş bir hızda tutmak doğru sonuçlar elde

etmek açısından önemlidir. Her iki kaliper tipi için dört farklı ivme ölçerden, 6 farklı kıstas için datalar toplanır.
Datalar toplanıp, dijital inputlara çevrilip, bilgisayara transferi yapılmıştır. Brüel&Kjaer programından elde edilen sonuçlar EXCEL programına aktarılıp, bu sonuçların grafikleri MATLAB ile çizilmiştir. Bulunan grafikler zaman kümesinde tanımlı grafiklerdir. Daha sonra bu zaman tanım kümesinde edilen grafiklerdeki tepe noktaları arasındaki genlikler, 6 farklı durum için her iki kaliper tipine göre tablo halinde bölüm sonunda gösterilmiştir.
Son olarak, deneysel ve matematiksel veriler karşılaştırılarak tartışılmıştır. Sonuç bölümünde benzerlikler ve farklılıklar saptanmaya çalışılmıştır. Matematiksel model ve deneylerde bulunan sonuçların paralellik gösterip gösterilmediğine bakılmıştır. Her iki yaklaşım için elde edilen verilerden çıkarımlar yapılmıştır. iki kaliper türü için titreşim farklılıkları bulunmuştur. Deneysel ve nümerik sonuçlarla örtüşmeyen değerleri nedenleri araştırılmış; bu farklı çıkan sonuçların sebepleri sıralanmış, bu farklılıklara öneriler getirilmiştir. Getirilen öneriler ışığında daha hassas sonuçlara ulaşılacağına kanaat getirilmiştir.

.

1. INTRODUCTION

The brake system in vehicles is used for inhibiting the motion. In today's world, most of the brake systems of the vehicles use the friction force between the surfaces to convert the kinetic energy into heat energy. The heat energy stored in the disc brake or drum during braking splits into air by itself. One of the biggest problems belonging to wheeled vehicles is brake noise problem, which is generated by friction force. Brake noise, vibration has been a problem, which receives great concern from the vehicle industries. Despite of the progress in technologies of the brake systems, there still exists a necessity to solve the brake vibration problems. It is so important to eliminate the brake noise for the vehicle comfort quality. The complexity of brake vibration dynamics is decreased day by day with the computer science in developing world. Owing to this, people have made great progress on brake vibration problems such as sequel, groan and brake judder etc.

The brake noise can be divided into three main categories: one of them is the high frequency (1-15 kHz) brake sequel, the second one is brake judder (below 100 Hz), and the third one is the mid frequency (200-500 Hz) brake groan.

1.1 Purpose of Thesis

The chief objective of thesis is to investigate the groan problem. The groan issue could occur particularly on vehicles with an automatic transmission when moving off because of simultaneous application of engine torque and release of brake pressure. The main reason of brake groan problem is known as stick-slip vibrations. Non-linear effect and the non-linear characteristics of friction coefficient is considered to be the cause of this vibrations. The goal of this project is to gain a better understanding related to the several system parameters which causes groan initiation.

There exists experimental studies and mathematical modeling in this project. The other aim of the project is to create a mathematical model by using governing equations. The governing equations will in the form of non-linear differential equations. Owing to generated numerical solution codes, the stability of the system for several parameters will be observed by linearized equations.

The another goal of the project is to build an experimental set-up. This experimental set-up enables to study stick-slip oscillations

1.2 Literature Review

The creep groan issue is investigated by Fuadi et al. [1] on a simple experimental model (caliper slider model). They investigated many parameters such as surface roughness of mating materials, properties of mating materials and structure's stiffness on brake groan problem. Z.Fuadi et al. [2] obtained a map by investigating a novel caliper slider experimental model. The map which is obtained demonstrates the necessary condition to avoid the generation of the creep groan problem of the brake system. The map describes the essential parameters such as stick-slip index, stiffness ratio to decrease the generation of the brake creep groan. Another study on creep groan is investigated by Abdelhamid [3]. This is also experimental investigation. Abdelhamid describes the creep groan problem which is occurred on the rear axles of the cars and light trucks and defines the limit cycles which are related to brake design and axle resonances in the motion of brake components.

Brecht et al. [4] found by using FE model that minimizing the difference between adhesion coefficient and dynamic friction coefficient have positive impact on brake groan. Moreover, he showed that adhesion coefficient and dynamic friction coefficient increase sharply as the friction components are wetted due to the rise of the creep groan intensity. Brecht et al.[5] used multi-body model to simulate brake creep groan. They developed a hypothesis to explain the effect of the friction material on brake creep groan problem by correlating the measured friction law with the results of road tests. It is proved that stick-slip oscillations are not only reason of the reason of brake creep groan problem, but also the mutual interaction of various component system affects it. Furthermore, it is stated that changing the one parameter of just a partial system cannot extinguish the stick slip impact because higher frequency stick slip movement occurs on unchanged partial system.

The friction torsional friction model of driveline and brake sub-systems is investigated by Crowther et al [6]. They formulate the groan problem into identical torsional-spring mass models with appropriate parameters derived from models with higher degrees of freedom for both manual and automatic transmissions. The model and numerical methodology is used to study sensitive parameters such as; inertia and frequency ratio, rate and magnitude of transient brake force, friction ratio etc. Crowther et al. [7] proposed both analytical and experimental investigations for an automatic transmission equipped vehicle. They made correlations between reductions in amplitude of friction force oscillations with reduced friction ratio by using brake test bench. They proposed new pad material formulations to give these characteristics. They concluded that the groan noise is structure-borne by observing the transmission losses in the airborne path.

It is shown by Hetzler et al. [8] that the system can undergo a subcritical Hopf-bifurcation from an unstable steady state fixed-point to an unstable limit cycle, which separates the basins of the stable steady state fixed-point and the self-sustained stick-slip limit cycle. It is found that, in contrast to squeal, a decaying friction characteristic may be a satisfying explanation for the onset low-frequency groan. The analytical results are compared with experimental measurements. Using an averaging method, the described stability properties are proven and the amplitude of the unstable limit cycle is quantified. Furthermore, the influence of the system parameters on the phase portrait is discussed.

Meng et al. [9] found that the increase of brake pressure and/or the decrease of brake disk's initial velocity, the tangent direction vibration was weakened, the variety of shape parameter has complicated nonlinear dynamics characteristics, while the normal direction vibration have no distinct changes. It is showed that the vibrations in the tangent directions intensify corresponding to the increase of brake pressure, and decrease as the relatively velocity excels certain values. Moreover, the varieties of shape parameter have complicated nonlinear dynamics characteristic.

1.3 Problem formulation

Fig.1.1 demonstrates the physical system in terms of a translating friction element with two different constraint locations. These cases simulate the push and pull type calipers respectively. Superscript T is used for trailing side parameters and superscript L is used for leading side parameters in the same way. The case (a) represents the push type caliper. Beside this, the case (b) simulates the pull type caliper. The difference between these two types of calipers is that the friction force

(F_f) between friction material (brake pad) and translating friction element pushes the friction material to the guide in push type caliper. On the other hand, the location of the constraint is at leading edge and friction force (F_f) pulls the frictional material to the frictional guide. There also exists a friction force, which is showed F_{fg} between the frictional material and frictional guide.

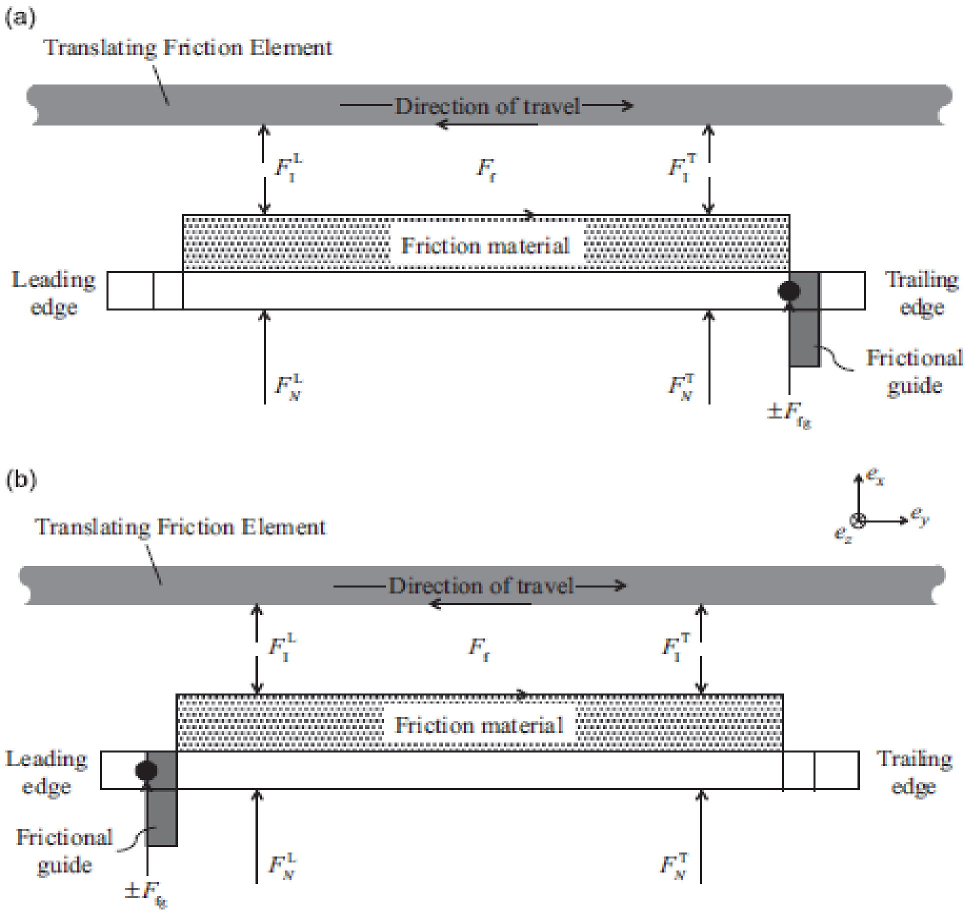

Figure 1.1: The general statement of the problem with translating friction element: (a) case frictional support at the trailing edge; (b) case with support at the leading edge [10].

F_N^L, F_N^T, F_I^L and F_I^T represents the normal and contact forces respectively at the leading and the trailing edge. Moreover, F_{fg} is the friction force between friction material and frictional guide surface. $\pm$ sign of F_{fg} depends on the positive and negative slipping velocity existing at supported edge.

Fig. 1.2 shows the possible normal load locations. The normal load can come from the close to the center or the supported edges. There exist three different cases in this thesis.

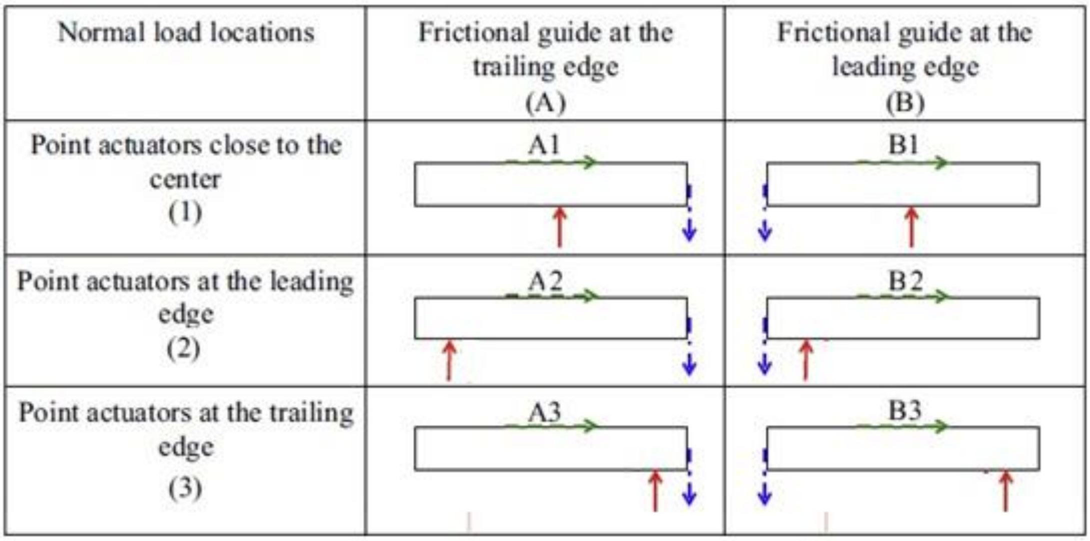

Figure 1.2: The loading and constraint direction, which will be examined in this thesis. Letter A represents trailing edge and Letter B represents leading edge. The normal load configuration is numbered.

Key: $\longrightarrow$ F_N^L and F_N^T ; $- - - \rightarrow$ F_f; $- \cdot - \cdot \rightarrow$ F_{fg} .

2. MATHEMATICAL MODEL

A minimal order model of the experiment has been developed. The simplified nonlinear and linear equations of translating friction element are obtained according to the cases given in Fig 1.2. In the experiment, the cases of Fig. 1.2 are obtained by varying the value of the parameter "β" as shown in the figures below. Based on the value of β, the location of the normal load is either at trailing edge, leading edge or center.

2.1 Governing Equations

Fig 2.1 and Fig 2.2 illustrate the nonlinear model of translating friction element problem. This nonlinear model has two degree of freedom. The translation (x) is only in the x direction and rotation (φ) is about z direction of the friction material. There exists no other rotation or translation in any directions.

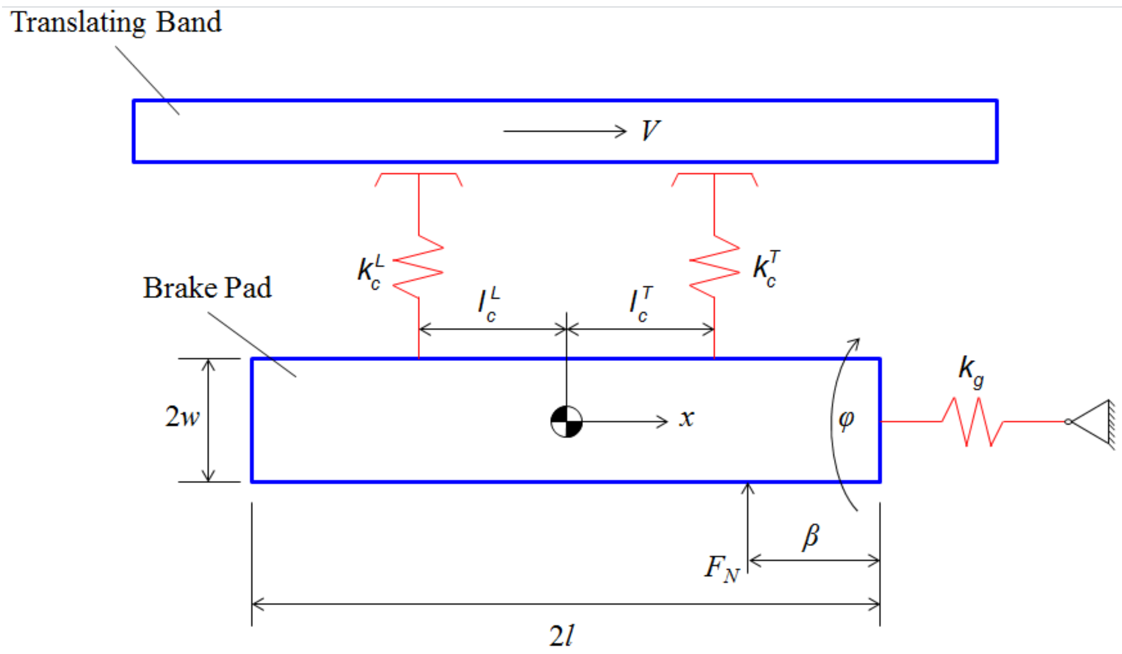

Figure 2.1 : Two degree of freedom nonlinear model of the translating friction element for push type caliper.

The contact forces are assumed to be linear springs. The linear spring coefficients of leading and trailing sides are k_c^L and k_c^T respectively. l_c^L is the distance of the contact force acting on leading edge between center of gravity. Conversely, l_c^T represents the distance between the contact force of the trailing side and CoG. The distance of normal force, which is applied on friction material, is shown as β. Furthermore, the length of the friction material is 2l and the width of the friction material equals to 2w.

Surely, there exists some nonlinearities such as contact loss between friction material and translating friction band interface and friction nonlinearity, which is generated by Stribeck type of friction model. However, it is just taken into account stick-slip nonlinearity, the other nonlinearities are neglected. Therefore, we just consider about two states. One of them is sticking regime. The second one is slipping regime. In sticking regime, friction material and translating friction band stick to each other. Thus, pad and friction band can be considered as a single rigid body, which moves together. In this case, the velocities belonging to the band and pad are equal in x direction. This equality in velocities neglects the equation in x direction. Therefore, the model turns into a single degree of freedom system.

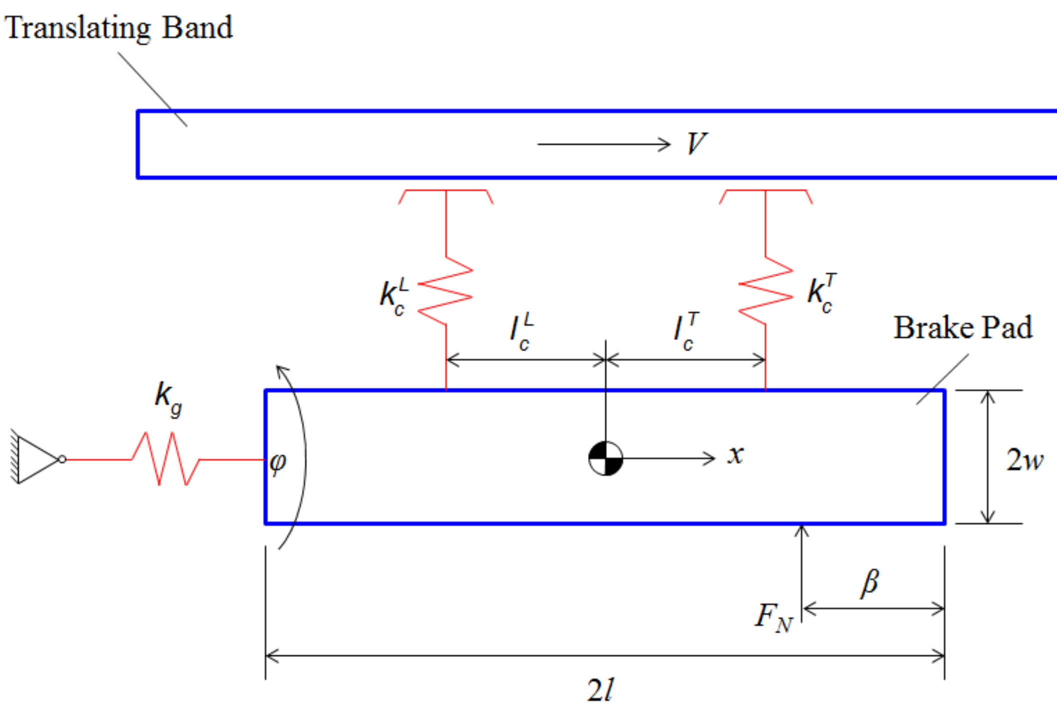

Figure 2.2 : Two degree of freedom nonlinear model of the translating friction element for pull type caliper.

Apart from the sticking regime, the relative velocity (V_r) between friction material and translating friction band does not equal to zero in slipping. Hence, we are not able to specify the velocity in x direction. Since the velocity in x direction is not known, the model should has two degree of freedom.

The relative velocity V_r can be written as following;

$$V_r = \dot{x} - V \tag{2.1}$$

We can write the governing equations by considering Fig. 2.1 for push type caliper in two cases(sticking and slipping) as below;

The governing equation for sticking case of push type caliper:

$$m\ddot{x} = 0 \tag{2.2}$$

$$I\ddot{\varphi} + k_c^L\left(l + l_c^L\right)^2\varphi + k_c^T\left(l - l_c^T\right)^2\varphi - k_g x w = F_N\beta \tag{2.3}$$

The governing equation for slipping case of push type caliper:

$$m\ddot{x} + k_g x + \mu(V_r)k_c^L\left(l + l_c^L\right)\varphi + \mu(V_r)k_c^T\left(l - l_c^T\right)\varphi = 0 \tag{2.4}$$

$$I\ddot{\varphi} + k_c^L\left(l + l_c^L\right)\left(l + l_c^L + \mu(V_r)w\right)\varphi + k_c^T\left(l - l_c^T\right)\left(l - l_c^T + \mu(V_r)w\right)\varphi = F_N\beta \tag{2.5}$$

The governing equations for pull type can be derived from Fig. 2.2. The governing equations for sticking case of pull type caliper are as following;

$$m\ddot{x} = 0 \tag{2.6}$$

$$I\ddot{\varphi} + k_c^L\left(l - l_c^L\right)^2\varphi + k_c^T\left(l + l_c^T\right)^2\varphi + k_g x w = F_N\left(2l - \beta\right) \tag{2.7}$$

In addition to the equations of sticking case, the governing equations belonging to slipping case are as following;

$$m\ddot{x} + k_g x + \mu(V_r)k_c^L\left(l - l_c^L\right)\varphi + \mu(V_r)k_c^T\left(l + l_c^T\right)\varphi = 0 \tag{2.8}$$

$$I\ddot{\varphi}+k_c^L\left(l-l_c^L\right)\left(l-l_c^L-\mu(V_r)w\right)\varphi+k_c^T\left(l+l_c^T\right)\left(l+l_c^T-\mu(V_r)w\right)\varphi=F_N\left(2\right. \quad \textbf{(2.9)}$$

The friction material depending on the direction of the friction force can either move faster than the band or move slower than the band. Therefore, the sticking conditions can be divided into two other states. Fig. 2.3 demonsrates the friction model which will be used according to these states.

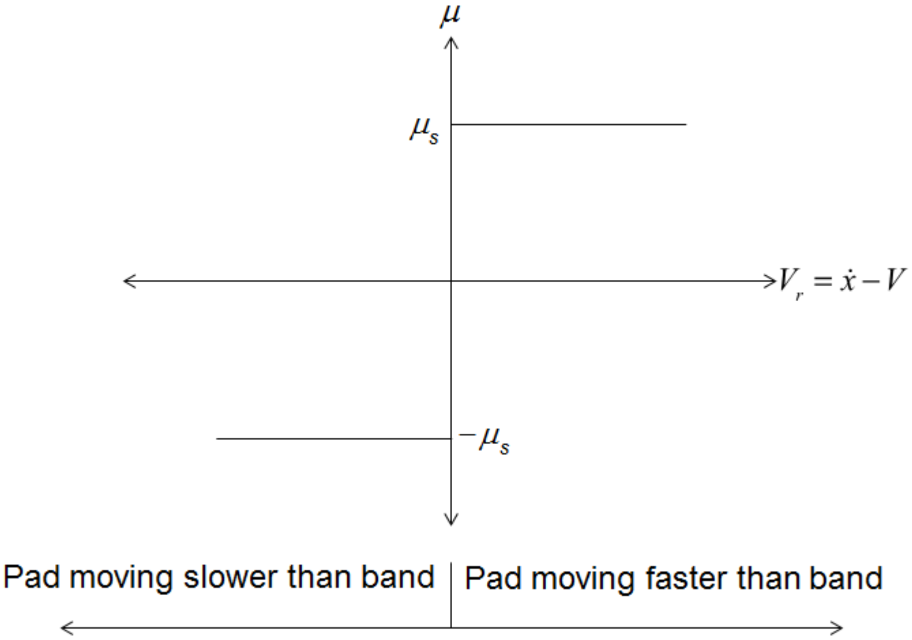

Figure 2.3 : Friction model to be used.

Beside the friction model which is to be used, the sign of friction coefficient changes according to the relative velocity of friction band. The friction band can move faster than the band or slower than the band. The friction coefficient which depends on the relative velocity (V_r) will be as following;

$$\mu(V_r) = \begin{cases} \mu_s & \text{for } V_r > 0 \\ -\mu_s & \text{for } V_r < 0 \end{cases} \quad \textbf{(2.10)}$$

2.2 Numerical Solutions

It is stated that there exists three states according to the relative velocity. Thus, the following four conditions, which should be considered, are demonstrated by Fig. 2.4 due to these three states.

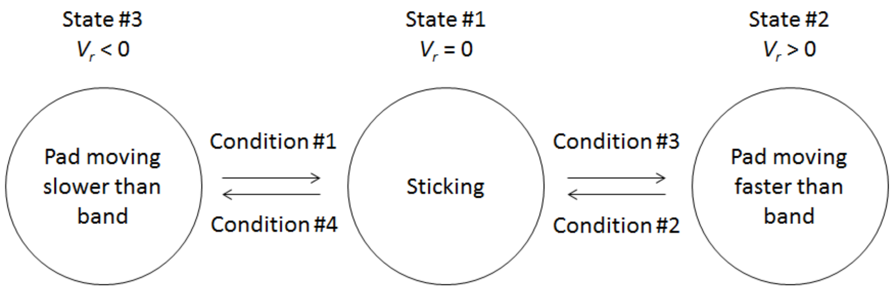

Figure 2.4 : The four conditions which depends on the relative velocity.

According to the these conditions, the governing equation for sticking condition (State#1) for push type caliper is written as below;

$$m\ddot{x} = 0 \tag{2.11}$$

$$I\ddot{\varphi} + k_c^L\left(l + l_c^L\right)^2 \varphi + k_c^T\left(l - l_c^T\right)^2 \varphi - k_g x w = F_N \beta \tag{2.12}$$

Governing equation for slipping case with pad moving faster than band (State #2) for push type caliper is in the form as below;

$$m\ddot{x} + k_g x + \mu_s k_c^L\left(l + l_c^L\right)\varphi + \mu_s k_c^T\left(l - l_c^T\right)\varphi = 0 \tag{2.13}$$

$$I\ddot{\varphi} + k_c^L\left(l + l_c^L\right)\left(l + l_c^L + \mu_s w\right)\varphi + k_c^T\left(l - l_c^T\right)\left(l - l_c^T + \mu_s w\right)\varphi = F_N \beta \tag{2.14}$$

Governing equation for slipping case with pad moving slower than band (State #3) is as following;

$$m\ddot{x} + k_g x - \mu_s k_c^L\left(l + l_c^L\right)\varphi - \mu_s k_c^T\left(l - l_c^T\right)\varphi = 0 \tag{2.15}$$

$$I\ddot{\varphi} + k_c^L\left(l + l_c^L\right)\left(l + l_c^L - \mu_s w\right)\varphi + k_c^T\left(l - l_c^T\right)\left(l - l_c^T - \mu_s w\right)\varphi = F_N \beta \tag{2.16}$$

The governing equation for sticking condition (State#1) for pull type caliper is written as below;

$$m\ddot{x} = 0 \tag{2.17}$$

$$I\ddot{\varphi} + k_c^L\left(l - l_c^L\right)^2 \varphi + k_c^T\left(l + l_c^T\right)^2 \varphi + k_g x w = F_N\left(2l - \beta\right) \tag{2.18}$$

Governing equation for slipping case with pad moving faster than band (State #2) for pull type caliper is in the form as below;

$$m\ddot{x}+k_g x+\mu_s k_c^L\left(l-l_c^L\right)\varphi+\mu_s k_c^T\left(l+l_c^T\right)\varphi=0 \tag{2.19}$$

$$I\ddot{\varphi}+k_c^L\left(l-l_c^L\right)\left(l-l_c^L-\mu_s w\right)\varphi+k_c^T\left(l+l_c^T\right)\left(l+l_c^T-\mu_s w\right)\varphi=F_N\left(2l-\beta\right) \tag{2.20}$$

Governing equation for slipping case with pad moving slower than band (State #3) is as following;

$$m\ddot{x}+k_g x-\mu_s k_c^L\left(l-l_c^L\right)\varphi-\mu_s k_c^T\left(l+l_c^T\right)\varphi=0 \tag{2.21}$$

$$I\ddot{\varphi}+k_c^L\left(l-l_c^L\right)\left(l-l_c^L+\mu_s w\right)\varphi+k_c^T\left(l+l_c^T\right)\left(l+l_c^T+\mu_s w\right)\varphi=F_N\left(2l-\beta\right) \tag{2.22}$$

In numerical solutions, the following condition should be tracked. The conditions for push type caliper are shown below:

Condition #1: $\dot{x}-V=0$

Condition #2: $\dot{x}-V=0$

Condition #3: $k_g x+\mu_s k_c^L\left(l+l_c^L\right)\varphi+\mu_s k_c^T\left(l-l_c^T\right)\varphi=0$

Condition #4: $k x-\mu k\left(l+l\right)\varphi-\mu k\left(l-l\right)\varphi=0$

The conditions for pull type caliper are shown below:

Condition #1: $\dot{x}-V=0$

Condition #2: $\dot{x}-V=0$

Condition #3: $k_g x+\mu_s k_c^L\left(l-l_c^L\right)\varphi+\mu_s k_c^T\left(l+l_c^T\right)\varphi=0$

Condition #4: $k_g x-\mu_s k_c^L\left(l+l_c^L\right)\varphi-\mu_s k_c^T\left(l-l_c^T\right)\varphi=0$

According to the numeric solutions, Fig. 2.5 demonsrates the time dependent displacement of the push type caliper. The graph is derived by simplifying the equations which are indicated above.

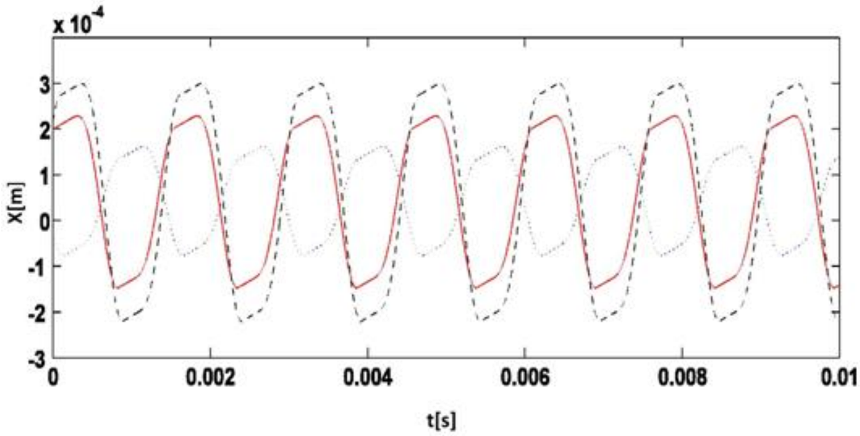

Figure 2.5 : Displacement-time graph of push type caliper.

The dashed long graphs of this section demonsrates as β equals 0,055. This means that the supported edge is close to leading side. The displacement magnitude of leading edge is bigger than the other ones. The graph of trailing side of which magnitude is less than the others shows the situation when β equals 0,025. These graphs which belong to trailing edge are showed with dashed short lines. The last graph which is showed by continuous lines represents the situation as the supported edge is close to the cente. The displacement magnitude size of it is between the other two graphs.

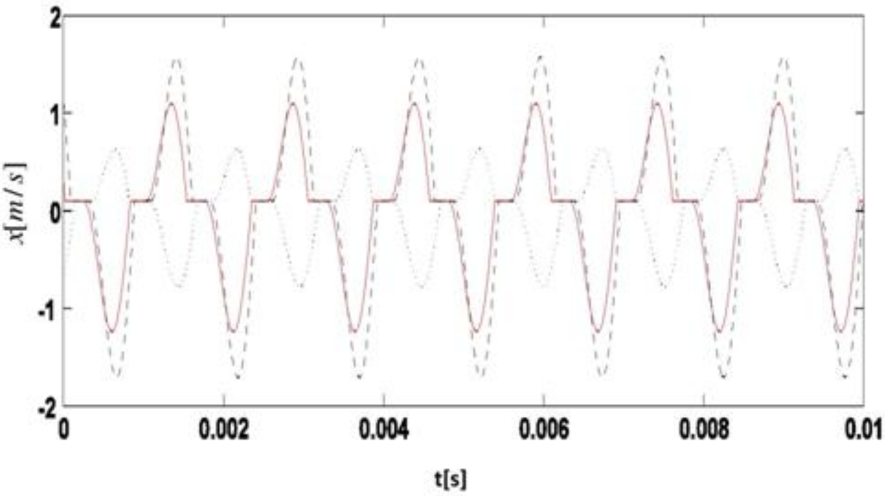

Figure 2.6 : Velocity-time graph of push type caliper.

According to this graph, the pad and band velocities are equal at a positive value which is approximately zero. After moving at the same speed, pad moves faster than the band. Then, the pad and band come up to same speed again. After moving a little more tine at constant speed, the pad starts to move slower than the band. The stick-slip are observed here.

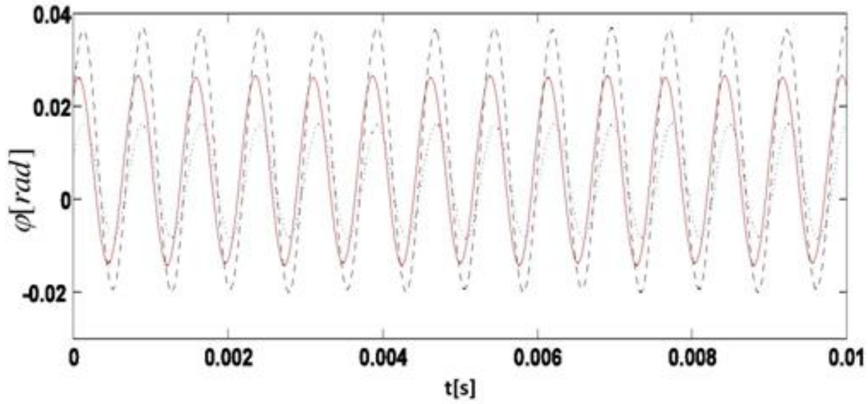

Figure 2.7 : Angular displacement-time graph of push type caliper.

The peak to peak values of angular displacement increases at leading edge where β equals 0,055. These values at close to center is between the values oof trailing and leading edge.

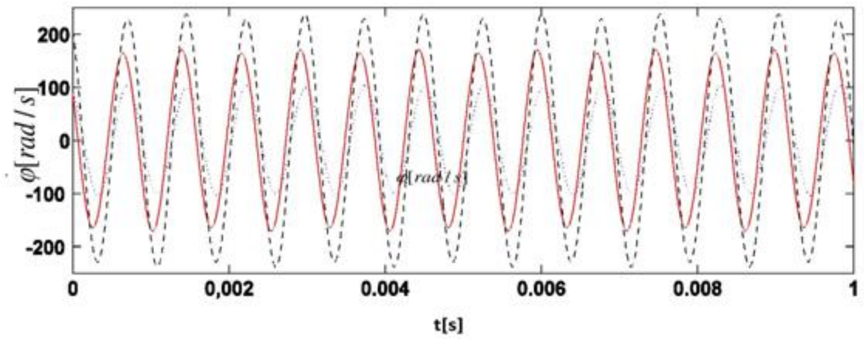

Figure 2.8 : Angular velocity-time graph of push type caliper.

The magnitude of angular velocity amplitude which belongs to leading edge is bigger when compared to center and trailing edge. The magnitude of trailing edge is the least one among them

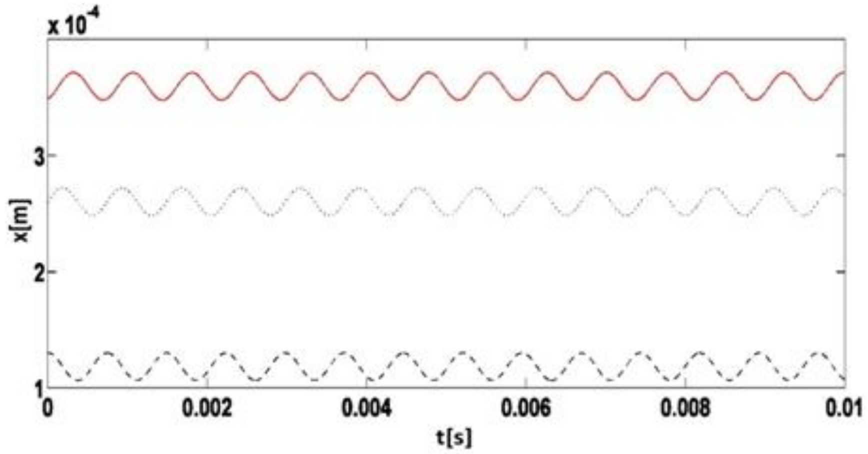

Figure 2.9 : Displacement-time graph of pull type caliper.

Displacement of pull type caliper has the biggest value where the supported edge is close to center. Apart from push type caliper, the magnitude of displacement is bigger at trailing edge.

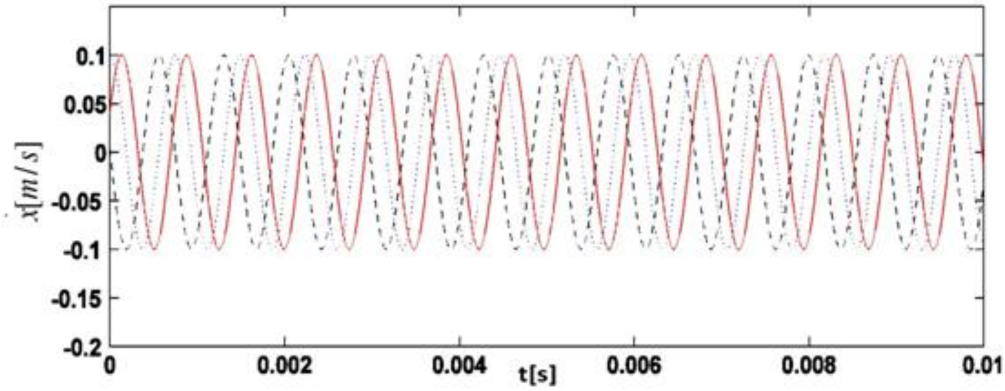

Figure 2.10 : Velocity-time graph of pull type caliper.

The velocity graph is different from the push type caliper. The magnitude of velocity amplitude is equal for all cases.

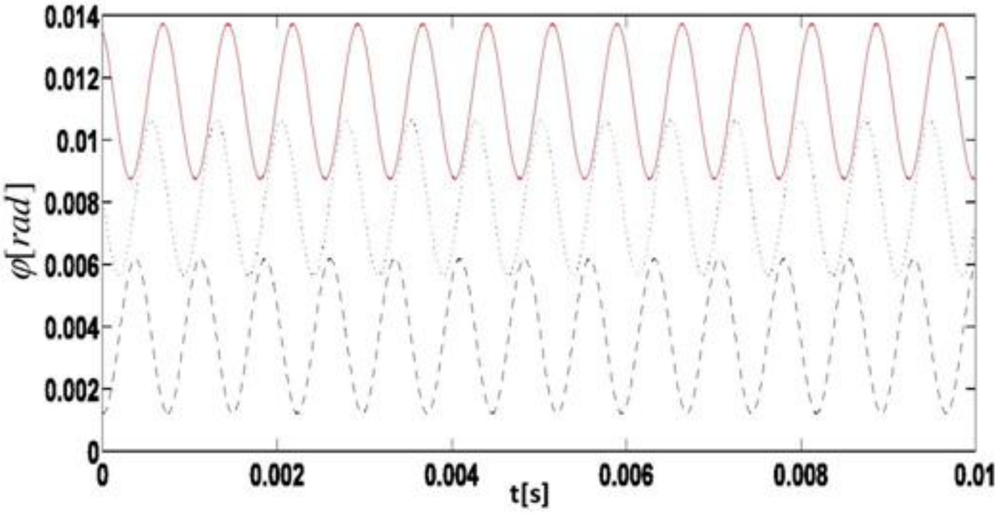

Figure 2.11 : Angular displacement-time graph of pull type caliper.

The magnitude of angular displacement has the biggest value at close to center. As we compare the trailing and leading sides, it is bigger at the trailing edge as linear displacement. The angular displacement-time graph is different for pull type caliper when compared to push type caliper. The peak points which belongs to three points (close to the center, trailing, leading) start and end at different regions apart from push type caliper type.

Fig 2.12 shows angular velocity-time graph which belongs to pull type caliper

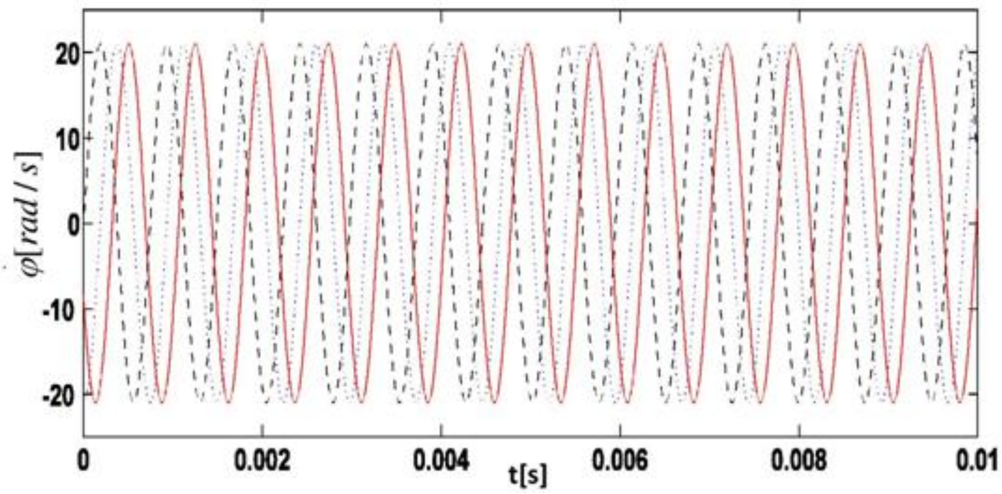

Figure 2.12 : Angular velocity-time graph of pull type caliper.

Angular velocities are equal for all cases. There is no difference between trailing, leading and close to center edges.

According to the data for the given graphs, peak to peak and mean values of push type and pull type calipers at close to trailing edge,center and leading edge are shown in Table 2.1 below.

Table 2.1 : Peak to peak values of push type and pull type calipers at close to trailing edge,center and leading edge.

		$x\,[m]$ x1000	$\dot{x}[m/s]$	$\varphi[rad]$	$\dot{\varphi}[rad/s]$
		pp	pp	pp	pp
PUSH	β=0.025	0,23713	1,7679	0,024435	202,27
	β=0.040	0.375	2,327	0,05557	333,1
	β=0.055	0,5164	3,269	0.05557	465,8
PULL	β=0.025	0,23713	1,7679	0,024435	202,27
	β=0.040	0,23713	2,327	0,0398	333,1
	β=0.055	0,5164	3,269	0,05557	465,8

3. EXPERIMENTAL STUDIES

3.1 Design Criteria

Experimental setup is designed to simulate both pull type and push type caliper. The direction of bracket should be changed with using screws to perform the translating friction element experiment for both type of calipers. Actuator can act from trailing side, leading side and close to the center as same as the states which is performed in the numerical solutions. Therefore, there exists six cases depending on the location of actuator for both pull type and push type caliper. Sen et. al [10] explain that frictional force decreases due to the increase on the rotational motion of brake pad when the location of actuation gets closer to the center of brake pad. Therefore, oscillations and the acceleration amplitudes are different according to the location of applied force. Stick-slip oscillations will be investigated according to the location of the applied force. The results which is obtained from the change on application point of the force can show the relationship between the location of applied force and stick slip oscillations.

3.2 Components

Experimental setup includes components such as pneumatic cylinders, friction band, the pad which is obtained from broken car, Teflon material, pneumatic hoses, compressors, electrical supply etc. According to this components, the experiment can be divided into three main categories as pneumatic line, mechanical system and electrical system. There exists measurement devices including accelerometers, manometers and data logger. There exists also frame which is a “U” shaped bracket that connects pneumatic actuator, teflon, brake pad and friction band. Fig. 3.1 demonstrates the schema of experimental setup. The point of frictional guide specifies the caliper type. The location of actuator is changed according to three states which is mentioned before.

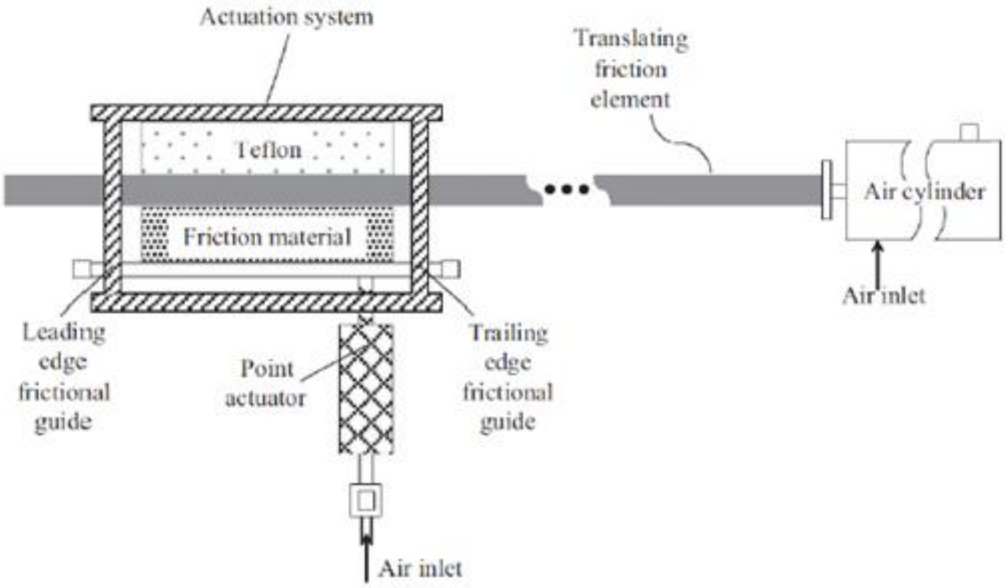

Figure 3.1 : Schematics of experimental setup [10].

3.2.1 Accelerometers

Brüel & Kjær ThetaShear® Type 4508 linear accelerometers are used in this experiment.The sensitivity which belongs to these accelerometers is 100 mV/g.The measuring range, frequency range are 700 m/s2, 1 Hz. – 8 kHz. respectively. One of the accelerometers is placed on the bracket on the friction band in the same direction with band. Another accelerometer is located on the friction pad in the same direction with pad (x direction). The other ones are located on the friction pad in the same direction with the pneumatic actuator (y direction).

3.2.2 Manometers

Manometers are supplied from FESTO. One manometer is located at the air inlet of big cylinder. The other one is located at the air inlet of pneumatic actuator.

3.2.3 Data logger

Brüel & Kjær is used for collecting data in this experiments. This data logger has four channels. These channels are connected to accelerometers which is replaced on different locations.

3.2.4 Friction band

It is manufactured from aluminium. It represents brake rotor. Therefore, the friction band should have a smooth surface like brake rotor in automobiles. Friction band is mounted on a big air pneumatic air cylinder. Friction band moves in the same axis with the brake pad.

3.2.5 Friction material

It is also called as friction pad. The pad is already obtained from an old car. It fits to frictional guides since it is machined before. We can observe stick-slip oscillations due to the friction which belongs to pad.

3.2.6 Pneumatic actuator

Pneumatic actuator behaves like a piston which belongs to a brake caliper. Pneumatic actuator applies normal force to brake pad. It moves horizontally according to the brake pad. The location of applied force is changed by moving pnuematic actuator to different supported edges horizontally.

3.2.7 Pneumatic cylinder

Pneumatic cylinder is used for moving friction band(brake rotor). Therefore, it is crucial component to examine stick-slip oscillations. Friction band is mounted on it with “L” shaped bracket.

3.2.8 Teflon

Since the friction coefficient is very low, the teflon material is preferred . The aim of usage is to assist during stick-slip examination. It is mounted at the rear side of friction pad.

3.2.9 Compressor

The compressor is used for suppling air to the friction element system during experimental stage. The air is given to the pneumatic cylinders with using appropriate fittings and polyamid hoses by compressor.

3.3 Experimental Stage

Experimental stage consists of design and experimentation stages.

3.3.1 The design and provision stage of the experiment

The brake pad is obtained from an old car. Brake pad base which belongs to pad is mounted with using three bolts. The friction band is obtained from aliminium material to have a smooth and clean surface. The frame which is an “U” shaped bracket is manufactured. Then, brake pad with base and friction band, teflon, pneumatic actuator is mounted on this frame. The compressor is connected with pneumatic actuator and cylinder with using “T” shaped fitting. The exists an accelerometer on friction band to measure the acceleration in x direction. The other accelerometer replaced on brake pad in same direction with pad to measure the acceleration in x direction. The other ones are perpendicular to brake pad to measure the accelerations of trailing, leading edges repectively in y direction. These accelerometer are connected to high precision cables which send the signal from sensor to computer when the experiment starts with the motion of pneumatic cylinders.

3.3.2 Experimentation

All throttles which belongs to pneumatic cylinders are closed at the beginning of the experiments. Thus, there is no air inlet from cylinders to the system initially. The pressure which comes from the compressor is approxiamately over 6 bar. The pressure of actuator is adjusted as 5 bar by using the throttle of the pneumatic actuator. Since the accelerometers are so sensitive, they can be influenced from any vibration acting on the system suddenly. Therefore, adjusting the pneumatic cylinder pressure is important to create more stable system and also to move friction band gradually. The friction band is started to move as the pressure which comes from pneumatic cylinder is between 0,6-0,7 bar. The analog signals are started to convert to digital inputs as the motion of the rod which belongs to pneumatic cylinder starts. It is important not to take overload results due to sudden signal which is caused by an incorrect motion of the band. Thus, it is crucial to keep the system at linear,slow speed to get positive results.

3.4 Experimental Results

The datas which are called disc_x, pad_x, pad_trail, pad_lead are obtained respectively owing to accelerometers which are connected to the system from different channels. Disc_x is the acceleration of disc in x direction. Pad_x is the acceleration of pad in x direction. Pad_trail and pad_lead is the acceleration of pad at trailing and leading edges repectively in y direction. The graphs can get close to zero as the velocities of pad and band are equal nearly. Because, the relative velocity is almost zero. As the pad and band stick , this means that pad and disc moves together, so there occurs no relative velocity.It is important to get the peak to peak values correctly to compare the graphs. Thus, the experiment is repeated three times for all 6 cases which are push_center, push_trail, push_lead, pull_center, pull_trail, pull_lead to get the correct results respectively. The feasible results are chosed from the saved document from these repeated tests. At the end, four datas for 6 cases are specified to observe the peak to peak values (Look at Table 3.1). For instance, Fig. 3.2, Fig. 3.3, Fig. 3.4, Fig. 3.5 are given below respectively to show the graphs of one case from 6 cases. These graphs belongs to leading condition of pull type caliper. X axis shows the time (s) and y axis shows the acceleration (m/s^2) on the graphs.

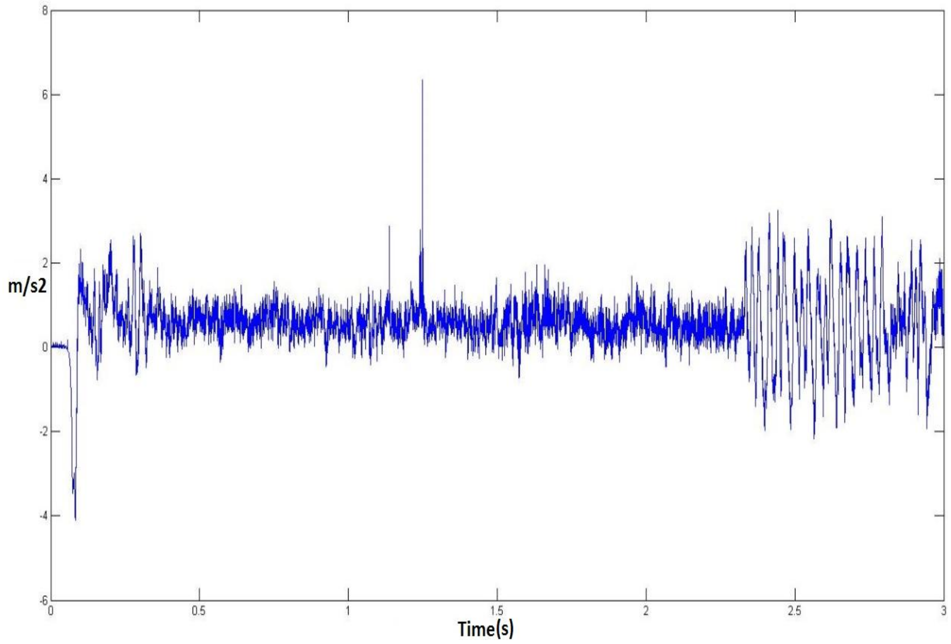

Figure 3.2 : The acceleration graph of friction band in x direction for pull type caliper.

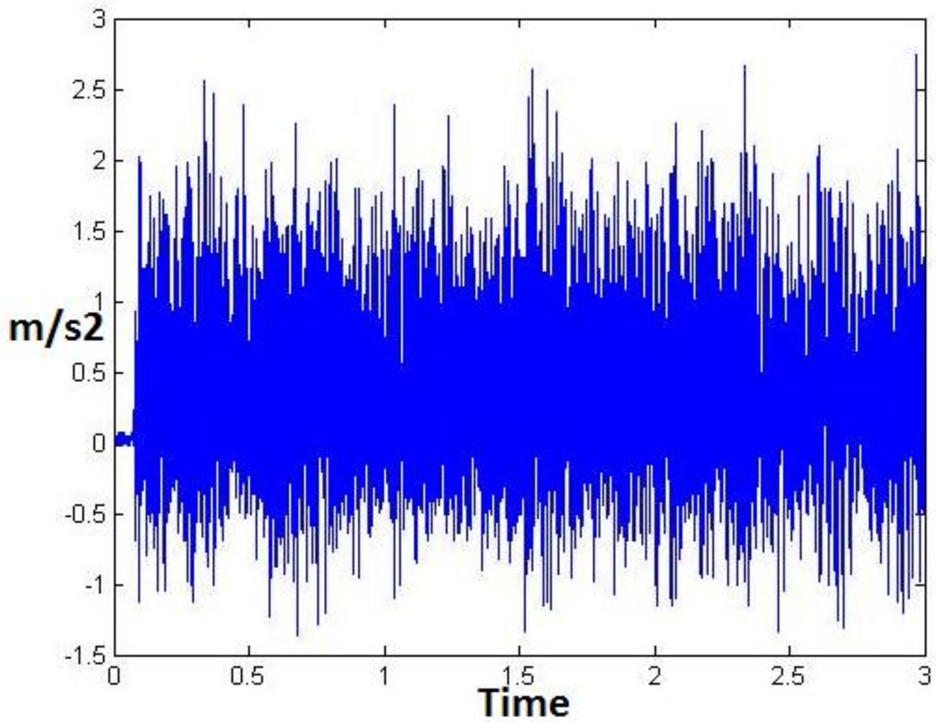

Figure 3.3 : The acceleration graph of friction pad in x direction for pull type caliper.

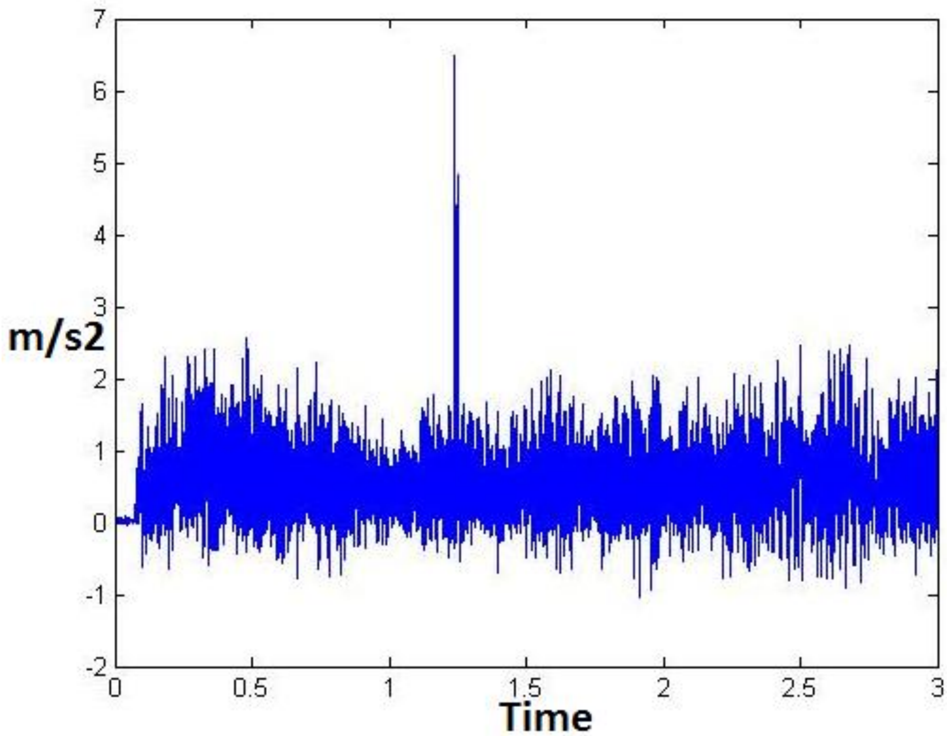

Figure 3.4 : The acceleration graph of trailing side of pad in ydirection for pull type caliper.

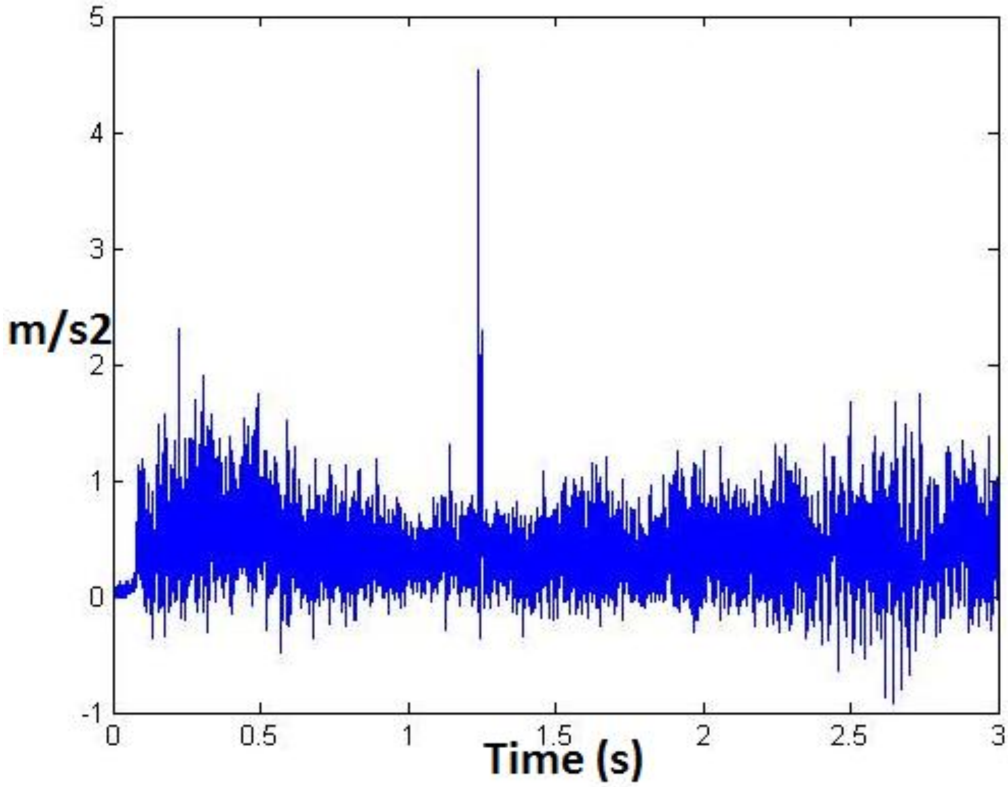

Figure 3.5 : The acceleration graph of leading side of pad in ydirection for pull type caliper.

Table 3.1 : Peak to peak values of acceleration amplitudes which is obtained from the experiment for 6 cases.

	disc_x	pad_x	pad_trail_	pad_lead
pull_center	1,6158	3,4109	1,7442	1,1799
pull_lead	1,846	3,488	1,338	0,891
pull_trail	1,949	3,411	1,692	1,356
push_center	1,846	2,744	2,077	1,77
push_lead	0,461	1,23	0,589	0,486
push_trail	3,975	3,975	2,437	3,306

4. CONCLUSIONS AND RECOMMENDATIONS

The aim of this project is to investigate the stick-slip oscillations, which cause groan initiation. A lower dimensional mathematical model is built. Since there exists nonlinearity in two-dimensional model, the model is simplified into one-dimensional model for numerical solution. Then, the graphs are obtained with writing numerical codes. In order to study the stick-slip oscillations, a simple yet controlled laboratory experiment is built. In this experiment, a custom-build friction material (that simulates the brake pad) is pushed against a translating brake band (that simulates the brake disc); hence a simpler version of brake system is designed. The graphs are drawn according to data that are collected from experiment. The results for both numerical solutions and experiment are written on the table for comparison.

In numerical results, the stick-slip oscillations are specified in push type caliper significantly. In can be seen that the amplitude of leading edge is the biggest one, then the amplitude of center comes and the amplitude of trail edge is the least one for both type calipers. There is no specific difference between the peak to peak values of push type and pull type calipers.

In experimental results, there exist significant differences between leading, trailing edges and center for push type caliper. The response of push type caliper changes faster depending on the location of the normal load. In pull type caliper, this change is not as obvious as push type caliper. The acceleration at trailing edge is bigger than the accelerations on other locations (leading edge) for both push type and pull type caliper. It can be said that the amplitude of center is bigger than the leading edge and the biggest amplitude is at trailing edge push type caliper. However, this gradation is not valid for pull type caliper.

Both results of numerical solution and experiment do not correlate exactly. One of the reasons of it is The mathematical model is simplified too much. The constant friction coefficient is assumed in the system and this not reflects the reality. The second reason can be the machining of the component are not adequate as it should be. Instead of precise machining for the components of the experiment, the spare and old parts found in the laboratory with simple or course machining processes are used. It is impossible to provide a constant velocity in experiment as it accepted in the mathematical model. The experiment is not a velocity-controlled type of experiment. The pneumatic forces are tried to adjust to a constant force. There exists an absence of instrumentation in experiment. The displacement of friction band and pneumatic pressures of pistons could not be measured.

To get more correct results, the components which belongs to experiment can be manufactured sensitively. Especially, the surface of friction band should be more smooth and more clean. The friction pad should have a homogenous surface profile. As indicated before, the displacements should be measured and controlled. A new degree of freedom to the band can be added for more clear results.

REFERENCES

[1] Fuadi, Z., Adachi, K., Ikeda H., Naito H., and Kato K. (2009). Experimental model for creep groan analysis, *Lubrication Science*, 27-40.

[2] Fuadi, Z., Maegawa, S., Nakano, K and Adachi, K. (2010). Map of low-frequency stick-slip of a creep groan, *Proceedings of the Institution of Mechanical Engineers, Part J: Journal of Engineering Tribology*, December 1.

[3] Abdelhamid, M., K. (n.d). Creep Groan of Disc Brakes, *AlliedSignal Automotive*

[4] Brecht, J., Hoffrichter, W., and Dohle, A. (1997). Mechanisms of Brake Creep Groan, *Textar GmbH*, pp. 79-85.

[5] Brecht, J., and Schiffner, K. (2001). Influence of Frıctıon Law on Brake-Creep Groan, *SAE INTERNATIONAL Proceedings of the 19th Annual Brake Colloquium & Exhibition (P-364)*, New Orleans, Lousiana, USA, October 28-31.

[6] Crowther, A., S., Yoon J., and Singh, R. (2007). An Explanation for Brake Groan Based on Coupled Brake-Driveline System Analysis, *SAE INTERNATIONAL*, Acoustics and Dynamics Laboratory, The Ohio State University.

[7] Crowther, A., S., and Singh, R. (2008). Identification and quantification of stick-slip induced brake groan events using experimental and analytical investigations, *Noise Control Eng. J. 56 (4)*, June 12, pp. 235-255.

[8] Hetzler, H., Schwarzer, D., and Seemann, W. (2007). Analytical investigation of steady-state stability and Hopf-bifurcations occurring in sliding friction oscillators with application to low-frequency disc brake noise, *Communications in Nonlinear Science and Numerical Simulation 12*, pp. 83-99.

[9] Meng, X., Wu, G., and He, L., (n.d). Numerical Study on the Vibration Characteristics of Automobile Brake Disk and Pad, College of Automotive Engineering Tongji University, Shanghai ,China.

[10] Sen, O., T., Dreyer, C.,T., and Singh, R. (2013). Low frequency dynamics of a translating friction element in the presence of frictional guides, as motivated by a brake vibration problem, *Journal of Sound and Vibration 332*, July 17, pp. 5766-5788.

APPENDICES

APPENDIX A: Technical Drawings

APPENDIX A

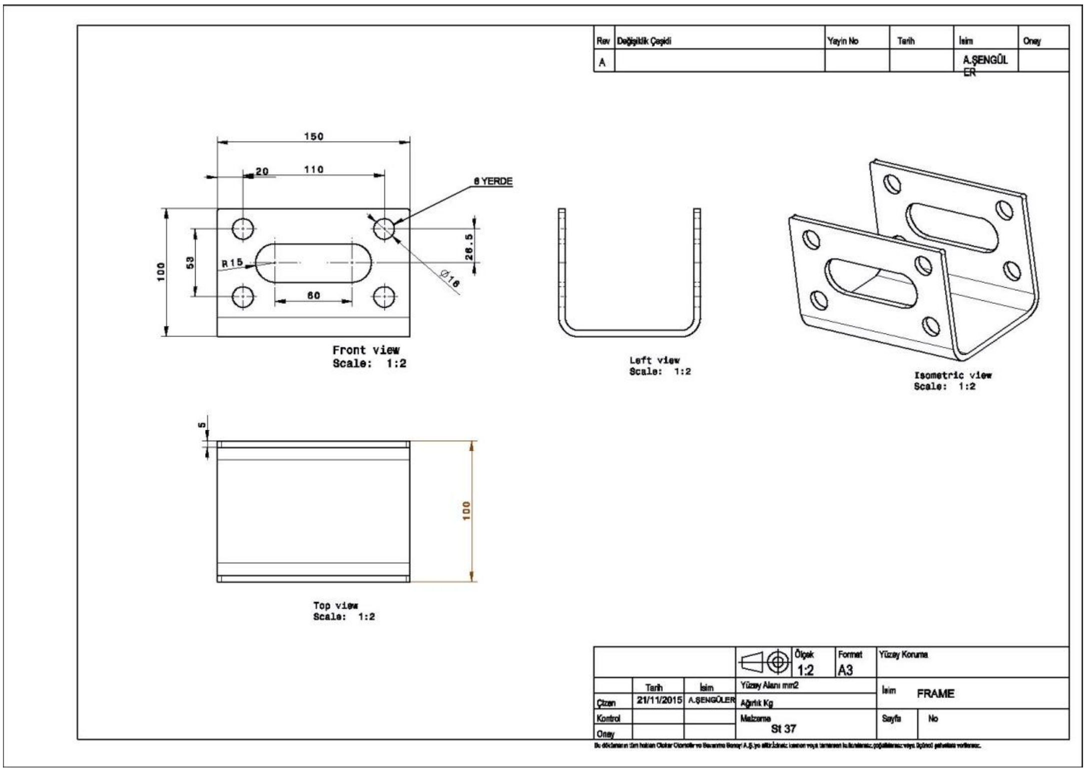

Figure A.1 : Frame.

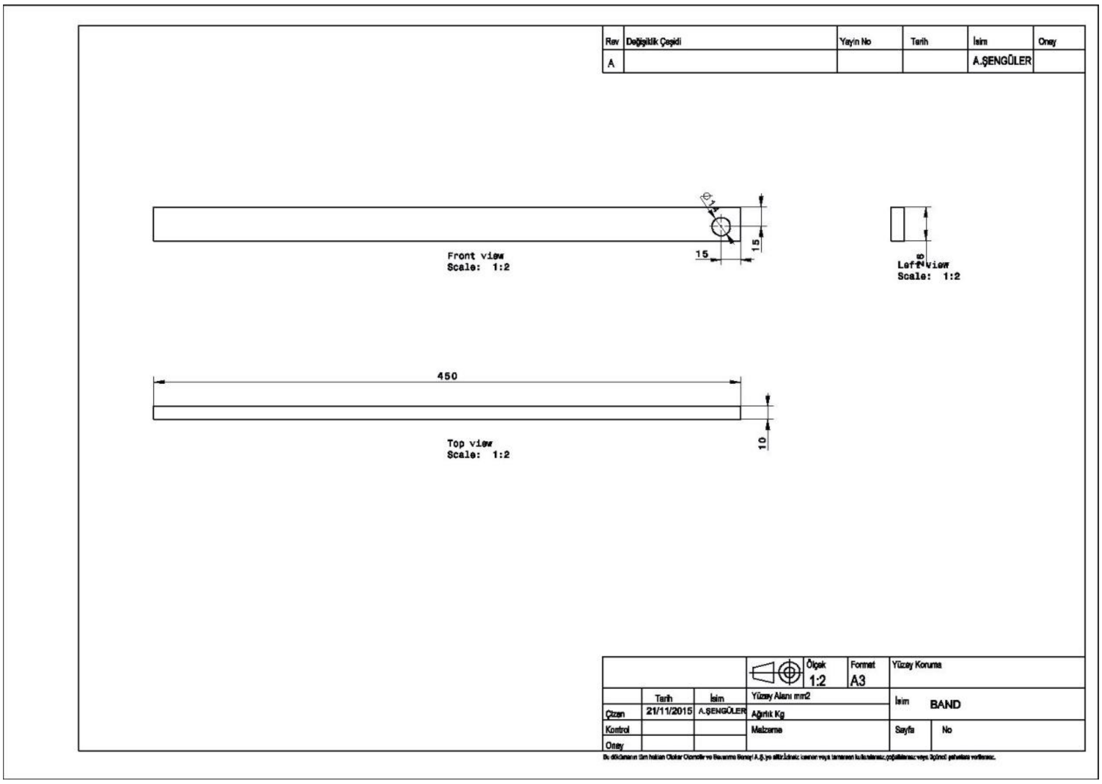

Figure A.2 : Friction band.

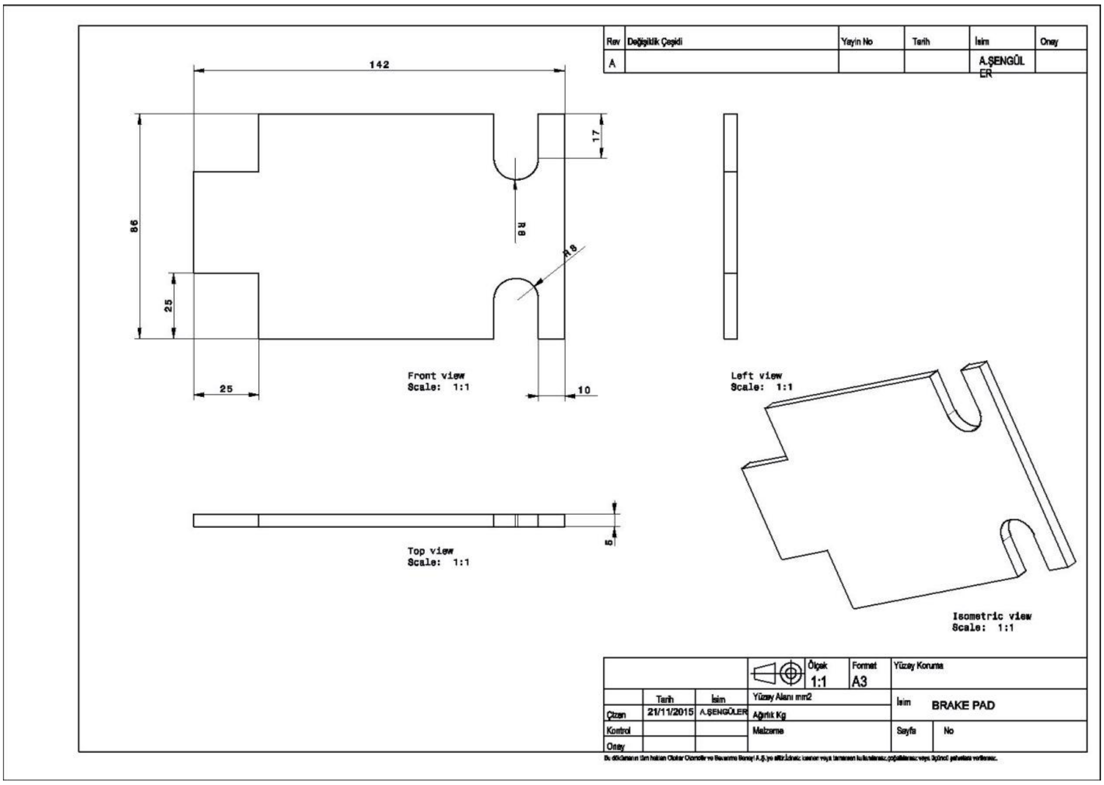

Figure A.3 : Friction pad.

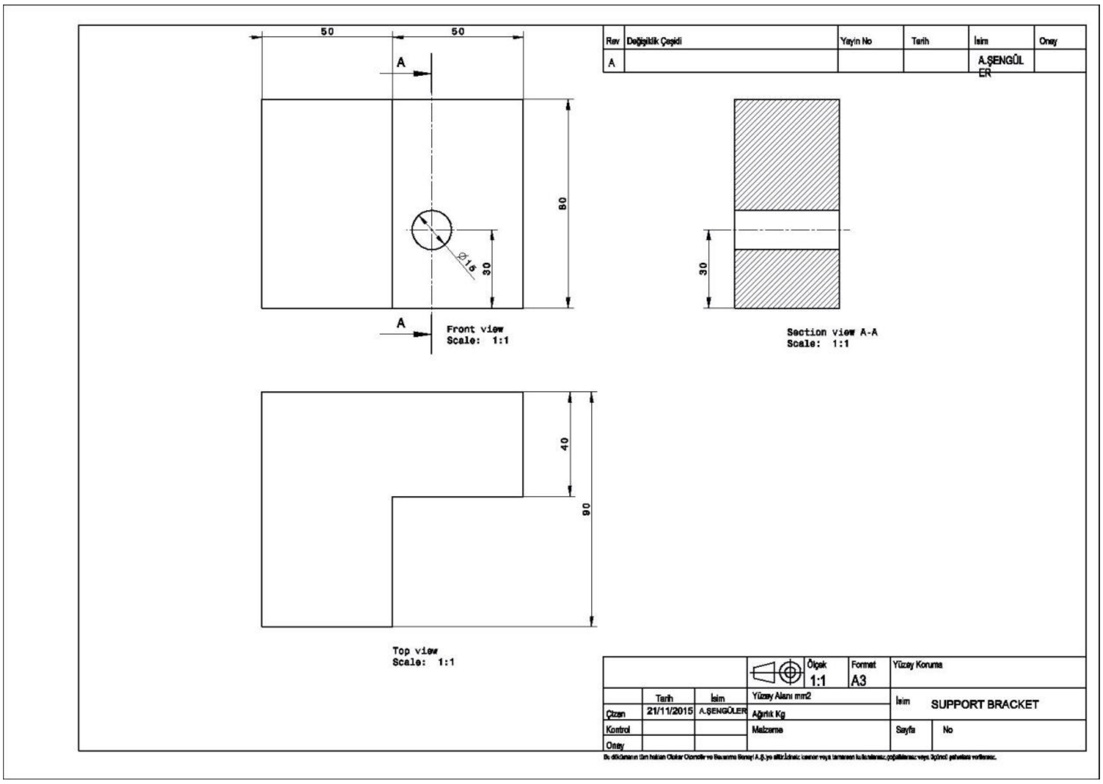

Figure A.4 : Support bracket.

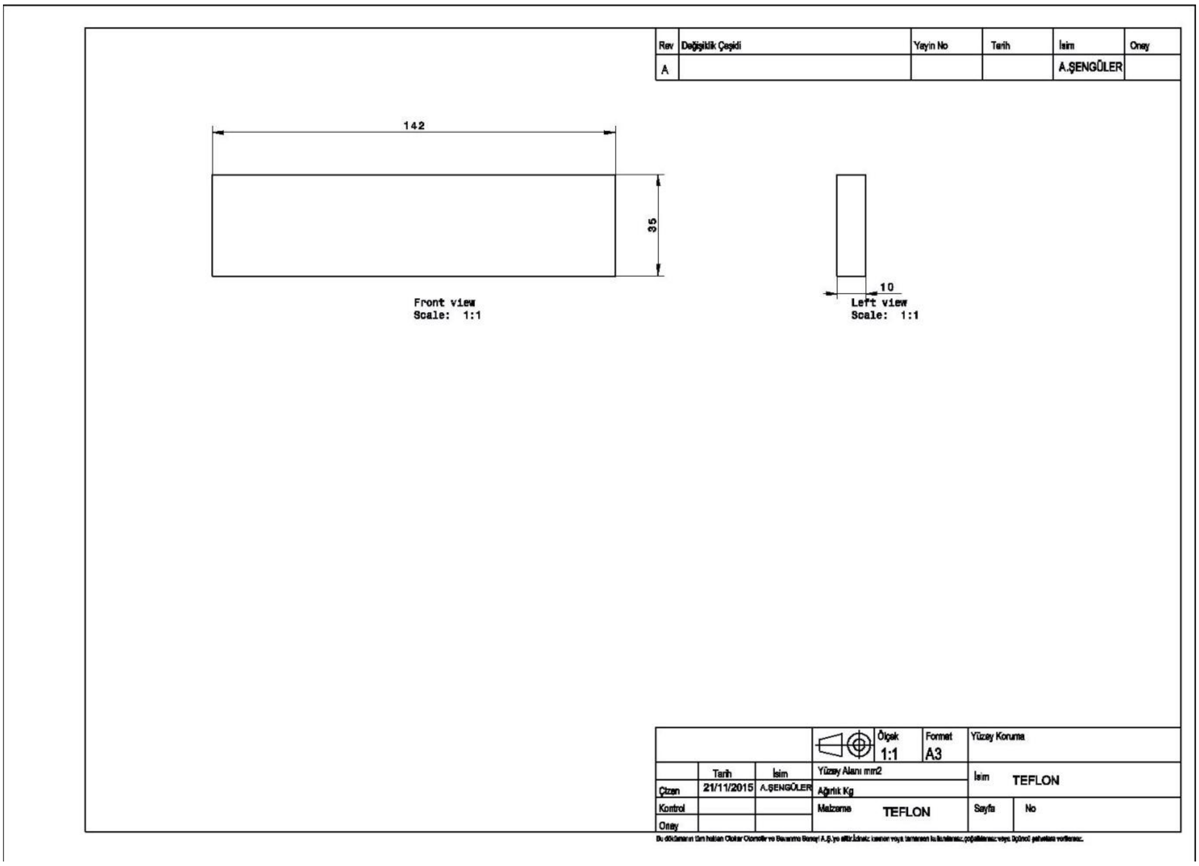

Figure A.5 : Teflon.

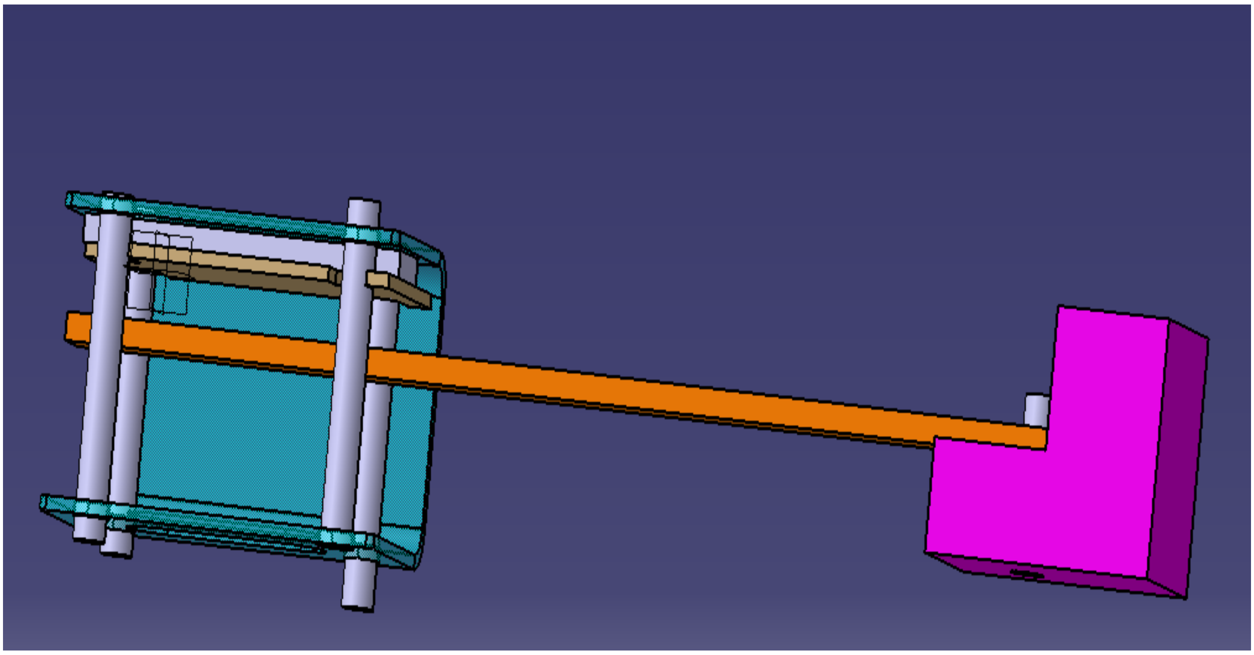

Figure A.6 : Assembly of friction element.

CURRICULUM VITAE

Name Surname: Anıl ŞENGÜLER

Place and Date of Birth: İSTANBUL-24.03.1989

E-Mail: anilsenguler89@gmail.com

EDUCATION: İstanbul Technical University

B.Sc.: Mechanical Engineering (2007-2012)

Experience:

2012-still	OTOKAR A.Ş-Chassis Development Engineer
2011	Mercedes-Benz A.Ş.-Intern

Computer Skills: CATIA, AutoCAD, SolidWork, C++, Microsoft Office 2010 / 2013 (Word, Excel, PowerPoint)